PROGRESS AND PERSPECTIVES OF ELECTRIC AIR TRANSPORT

H. Kuhn, A. Seitz, L. Lorenz, A.T. Isikveren, A. Sizmann
Bauhaus Luftfahrt e.V., Lyonel-Feininger-Str. 28, 80807 Munich, Germany
holger.kuhn@bauhaus-luftfahrt.net; arne.seitz@bauhaus-luftfahrt.net; larissa.lorenz@bauhaus-luftfahrt.net; askin.isikveren@bauhaus-luftfahrt.net; andreas.sizmann@bauhaus-luftfahrt.net

Keywords: *electric motive power systems, Ragone metrics, exergy concept, electric flying*

Abstract

We address the expediency and explore the innovation potential of Hybrid Electric Power Architectures (HEPAs) in aviation. As a starting point, we define three fundamental principles for the feasibility assessment of electric flight and introduce the Ragone metrics as essential analytical parameters. Following a discussion of key system components and their technology perspectives, we describe four examples of HEPA systems, including the Universally-Electric System Architecture (U-ESA), which realizes zero in-flight emissions. The significant loss in aircraft range brought about by the high weight of U-ESA components can –in view of present technology options– only be counteracted by providing part of the aircraft's power demand with a conventional turbo-engine. We analyse this 'battery + fuel' hybrid system in detail and draw interesting conclusions about the impact of the degree of hybridization on aircraft range, energy consumption and CO_2 emissions.

1 Introduction

Future growth of the aviation industry will depend crucially on the reduction of its environmental footprint through substantial efficiency gains and substitution of fossil kerosene by renewable alternatives [1–3]. The universally electric aircraft is the most radical step in this direction: If battery-powered, such an aircraft would have zero in-flight emissions, surpassing even the ambitious Flightpath 2050 [4] goals of 75% reduction in CO_2 and 90% less NO_x. The flexibility in choosing the primary source of electric energy paves the road to long-term sustainability and a low overall emission budget through the use of power from solar radiation, wind, water or geo-thermal sources.

The electric aircraft concept also offers the possibility to optimize aircraft efficiency using radically different configurations, due to the new degrees of freedom released by the separation of power generation from power consumption. Aerodynamic as well as propulsive efficiency can benefit from the liberty of integration offered by universally or hybrid electric power systems, as can control dynamics, service accessibility, and mass and load distribution. Together with the future technology perspectives of electric components and sub-systems, these advances in configuration and propulsion integration can potentially yield the step changes in efficiency and emission necessary to ensure sustainable long-term growth for the aviation sector.

In this paper, we first address the fundamental feasibility and scaling properties of electric flight, highlighting the importance of properly defined system boundaries and introducing the Ragone diagram as the key tool for system comparison. We then take stock of the various technologies required to set up Hybrid Electric Power Architectures (HEPA) and discuss their potential for future development. We illustrate four distinct system architectures: an entirely battery-powered system, a fuel cell system and their hybrid combination, i.e. three options for a Universally-Electric System Architecture (U-ESA); and a hybrid of a conventional turbo-engine and battery. The performance of a U-ESA is then analyzed in the context of concrete future mission requirements [5]. Finally, we present a detailed study of the possible range extensions for an U-ESA platform in hybrid combination with a conventional turbo-engine: Introducing the Degree of Hybridization (DoH) as a key parameter, we show how energy consumption and CO_2 emissions per passenger-kilometer vary with DoH, concluding that a given target for emission reduction –such as set by the EU in the Flightpath 2050 report [4]– essentially dictates a minimum amount of hybridization for the power system.

2 Feasibility and Scaling Properties of Electric Flight

A major challenge for electric flight lies at the interface between scientific principles and developments related to electro-mobility outside the field of aviation, and aviation-specific questions such as (novel) aircraft configurations and optimal system integration. Only a successful combination of both aspects will allow to exploit their full potential for innovation. Here, we set the stage by introducing the underlying guidelines and parameters for our subsequent analysis.

2.1 Principles of the Feasibility Assessment of Electric Flight

Three fundamental principles of the feasibility assessment of electric flight as proposed by Bauhaus Luftfahrt are [2, 3]:

1. *Exergy concept:* The usefulness of an energy carrier for aviation is determined by its specific exergy content, i.e. gravimetric and volumetric exergy density, rather than by its energy content.

2. *Specific power and Ragone metrics:* The usefulness of an energy carrier in combination with a power converter is fundamentally determined by their combined power density and exergy density (Ragone metrics). These two metrics are the key indicators for electric aircraft feasibility when comparing alternative power sources.

3. *Hybridization degrees of freedom:* Two or more energy storage and power conversion devices that separately are inadequate for electric flight (according to their Ragone metrics) may constitute an enabling power system when combined into a hybrid system.

Each subsequent principle adds to the previous one an essential and new dimension in the feasibility assessment of electric flight. We now discuss the significance of these principles in detail.

The first principle is based on the second law of thermodynamics and relates the fact that exergy is the part of the energy that can absolutely be converted into useful work. The net exergy of a given system is determined by the sequence of conversion efficiencies in each of its individual components. Note that, unlike universally electric power systems, combustion engines are fundamentally limited by the Carnot efficiency. Therefore, the huge apparent energy density gap between kerosene and state-of-the-art batteries for electromobility (a factor of 50 to 60) is reduced to a factor of 20-30 when one accounts for the absence of the Carnot limitation in non-thermal electric power conversion.

According to the second principle, the feasibility of electric flying is best understood in terms of the Ragone diagram as shown in Fig. 1. A high energy or exergy density, such as it is associated, e.g., with hydrogen-powered fuel cell systems, is an insufficient (and even misleading) indicator for the capability to realize electric flight because the specific power requirements of take-off and climb have to be met at the same time.

These requirements are increasingly difficult to fulfill for larger aircraft take-off masses. In some cases the limitations of fuel cell systems are best overcome by including an auxiliary high-power-density battery system. Hence, a hybrid system as advocated by the third principle can meet the power and energy requirements expressed in terms of the Ragone metrics even though the indivdual subsystems show inadequate performance characteristics.

2.2 System Boundaries and Ragone Representation

The exergy densities and power densities of two exemplary motive power systems are displayed in the Ragone diagram of Fig. 1. 'Battery+Motor' denotes a universally battery powered system with electric motor (dashed light blue line), while 'FC+BoP+H2+Tank+Motor' refers to a fuel cell system (BoP: Balance of Plant) powering an electric motor (using a liquid hydrogen tank as an energy source, solid green line). Also depicted is the Ragone representation of typical medium-range aircraft with conventional turbo-engine: The points A,B,C (orange triangles) correspond to selected points on the aircraft's payload-range diagram (compare inset plot in Fig. 1). During a typical mission, the aircraft will follow the solid orange line starting in point A. Note that A and B are very close, and that the aircraft 'crosses' the U-ESA ('Battery+Motor') performance line while passing from point B to the state where only reserve fuel is left in the tank (point C).

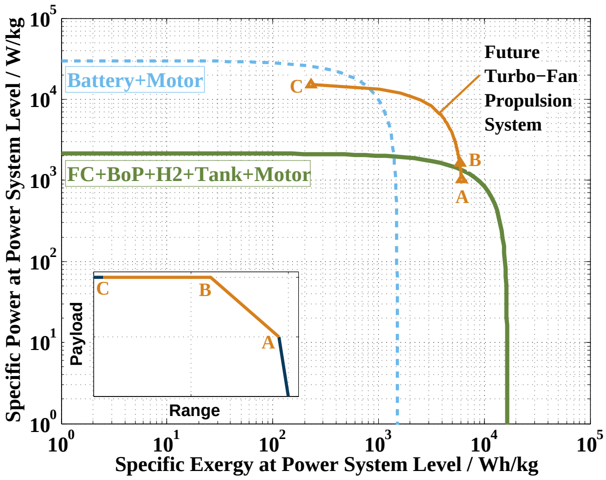

Fig. 1 Ragone diagram presentation (specific exergy [Wh/kg] vs. specific power [W/kg]) of different HEPA systems and the 'Ragone range' of the payload-range diagram of a future medium range aircraft (see inset plot). Data from Table 1.

Table 1 Characteristic values for the power system components.

Component	Unit	2010	2035+
Kerosene	kWh/kg	11.9 [a]	
Hydrogen	kWh/kg	33.31 [a]	
Fuel tank	kg	– [b]	
Lithium battery	kWh/kg	0.60	1.5
Turbo-engine [c]	kW/kg	15.0	18.0
Fuel cell (PEFC) [d]	kW/kg	1.2	3.0
Percentage of BoP [e]		0.40	0.30
Generator	kW/kg	10.0	20.0
Motor	kW/kg	10.0	20.0
Power management [f]	kW/kg	10.0	15.0
Efficiencies		**2010**	**2035+**
Turbo-engine		0.50	0.55
Fuel cell		0.50	0.65
Generator		0.99	0.99
Motor		0.99	0.99
Power management		0.95	0.98

[a] Lower Heating Value (LHV)
[b] The mass of the fuel tanks are calculated separately depending on the fuel amount.
[c] bare turbo-shaft specific power at max power
[d] PEFC: Polymer Electrolyte Fuel Cell
[e] BoP: Balance of Plant
[f] single system without redundancies

2.3 Architectures and Combinations

The power systems plotted in Fig. 1 are only two among a variety of architectures that are possible for HEPA systems. In principle, the HEPA concept includes all system combinations that can be formed with the various sources of energy and types of power converters in Fig. 2. 'PMAD' in Fig. 2 stands for Power Management and Distribution System, i.e. the components that establish the essential link between power generation and consumption in the turbine. The performance characteristics for each system are listed in Table 1. These numbers are the basis for the calculations presented in the later sections of this paper.

A useful exergy analysis of these systems requires a proper identification system boundaries and estimate of conversion efficiencies. Furthermore, the scaling behaviour and feasibility assessment requires the Breguet and the Specific Breguet Range equations to be adjusted to electric battery power release without change in mass. These aspects have been carefully considered when establishing the systems' representation in the Ragone diagram of Fig. 1.

3 Future Perspectives of Key Technologies

For an accurate evaluation of the feasibility, progress and perspectives of universally electric and hybrid motive power systems a physics-based fundamental understanding and modeling approach of the basic components is mandatory. We therefore examine the prospects of key technologies relevant for electric flight – such as batteries, fuel cells, motors and generators –, pointing out selected scientific and technical limits on their future development.

3.1 Batteries

Today, standard electrode materials such as lithium metal oxides $LiMO_2$ (M = Co, Mn, FePO) and graphite (C) limit the specific energy of commercial batteries to a level below 300 Wh/kg. Nevertheless, existing batteries have been demonstrated to serve as the main source in small light airplanes enabling flight times of up to 3 hours.

Crucial battery components with significant innovation potential are the electrodes and the electrolyte. Therefore a range of new electrode materials is under investigation promising significant higher capacities as well as charge-discharge rates. As stated elsewhere, the specific power is as important as the specific energy in order to provide high power capabilities at high energy storage levels to allow for electric flight [2].

Recent developments and laboratory-scale demonstrations in electrode materials prove promising performance enhancements of secondary batteries that could result in a significant step change regarding energy and power densities. Kang *et al.* demonstrated very high discharge rates for lithium phosphate coated $LiFePO_4$ electrodes allowing for a full charge between <2 and 30 minutes at reasonable specific capacities of 130 to 170 mAh/g, respectively [6]. LiNiMnCo oxide electrodes are another promising class of positive electrodes. Ban *et al.* demonstrated charge-discharge cycles at 5 C (full charge in 12 minutes) at reasonable capacities of 120 mAh/g after 500 cycles, whereas at 10 C (6 minutes) still capacities of 110 mAh/g after 500 cycles are feasible [7]. For comparison, standard $LiCoO_2$ electrodes exhibit a capacity of less than 135 mAh/g at rates below 1 C (1 hour). Sulphur has a theoretical capacity of 1166 mAh/g which is far beyond the capacities of the previous discussed materials and is therefore a promising material. The drawbacks of sulphur are its insulation characteristics and large volume changes upon lithium insertion/extraction. Electric conducting additives such as carbon need to be added, hence reducing the specific capacity. The volume changes may be overcome by nano-structuring of the electrode. Yang *et al.* realised a cell incorporating a lithium-sulphur carbon composite electrode having a specific energy of 315 Wh/kg at battery level [8].

To enhance the performance capabilities of a battery both electrodes need to be optimised in terms of specific charge and rate capability. Compared to the positive electrode there are more materials under investigation for the negative electrode such as silicon as the most popular today due to the theoretical specific capacity of 4200 mAh/g and significant improvements in nano-structuring [9–13]. Chan *et al.* demonstrated capacities between 2100 and 3500 mAh/g for silicon nanowires at discharge rates of 1 C to 1/5 C, respectively. For comparison standard graphite electrodes exhibit a capacity of 350 mAh/g at similar charge-discharge rates.

In the past, the specific energies of batteries increased by 7 % per year by optimising standard electrode materials and their structure. According to the maximum theoretical capacities of the electrode materials this trend will not continue due to physico-chemical limits of the materials. We set up an electrode inventory comprising 9 positive and 20 negative electrode materials and investigated all possible combinations of these electrodes in order to identify their potentials of specific energy with respect to equilibrium potential, molar mass

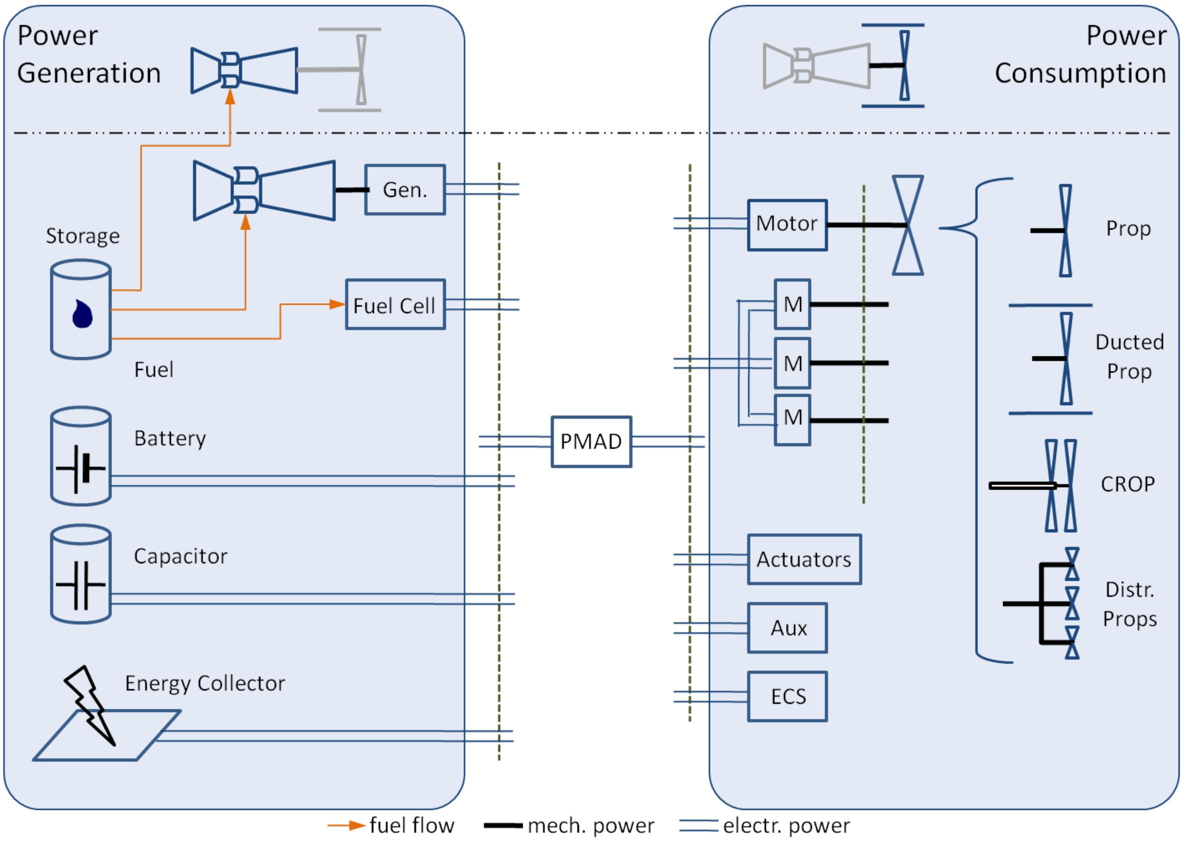

Fig. 2 Components for power generation (left) and power consumption (right) from which a combinatorial variety of electric power architectures can be derived.

and reversible range [14]. Specific energies in the range of 1000 to 1500 Wh/kg seem to be feasible in the mid to long term time horizon which is 5 to 7 times the specific energies of commercial batteries today.

3.2 Fuel Cells

Polymer electrolyte fuel cells (PEFC) are considered as possible power generators because of the advantage of using high energy density liquid hydrogen in combination with a high fuel-to-electricity conversion efficiency. PEFCs provide a specific power of up to 1.25 kW/kg (at stack level), the highest among all fuel cell technologies. A study by Middelman *et al.* shows that specific powers of 2 kW/kg at stack level are feasible in the near term [15] by improving bipolar plate characteristics, the main contributor to weight and volume of the stack.

Platinum is still the main catalyst for fuel cell electrodes. The platinum loading greatly reduced from initially 4 mg/cm^2 to 0.3 mg/cm^2 retaining same or enhanced power capabilities at significantly reduced costs. Regarding the CO intolerance of platinum it is of major importance to remove any traces from the operating gases. New catalysts such as platinum supported on a TiWO substrate exhibit higher tolerance levels towards CO [16]. Core-shell Pd/FePt nanoparticles serve as alternative catalysts for the oxygen reduction reaction (ORR) [17]. These new catalysts materials allow for enhancing the durability, stability and cost of PEFCs.

Nafion is the state-of-the-art membrane for PEFC. These membranes need to be humidified in order to conduct hydrogen ions and therefore the humidity management of a PEFC is crucial for its power capabilities. Based on alternative silicon membranes the humidity management may be significantly simplified, hence reducing balance of plant requirements [18]. Increased ionic conductivity further reduces internal losses and hence increases specific power of the PEFC stack.

Considering improvements in catalyst loading (less catalyst per area), higher ionic conductivity based on alternative membranes (less internal losses) and enhanced bipolar plates the specific power of PEFC may be in the range of 2 to 3 kW/kg in the future.

3.3 Electric Motors

The third key component is the electric motor producing shaft power to drive the propulsor. Normal-conducting motors have specific powers in the range of 2 to 10 kW/kg, entering the power density domain of turbo-engines.

Power density prospects of high-temperature superconducting (HTS) motors as high as 40 kW/kg, i.e. well above the level of state-of-the-art turbo-engines, have been reported [19]. A physics-based model, extended to the superconducting regime, will provide a future-proof framework for power and mass scaling of HTS electric motors, and analogously of generators for turbo-electric systems as well.

4 Electric Power System Architectures

Among the choices illustrated in Fig. 2, we now discuss four power system examples in more detail, highlighting their advantages and challenges. The universally-electric battery system (Section 4.1) and its hybrid with a conventional turbo-engine (Section 4.4) will be studied in a concrete integration example in the next two sections.

4.1 Battery System

A typical battery-powered U-ESA is shown in Fig. 3; note that energy storage and conversion are combined inside the battery, making it the system with the least number of components. Two different types of batteries, which can be used in (parallel) combination, are indicated, namely high energy density-optimized batteries (‘E’) and their high power density counterpart (‘P’). Unlike conventional turbo-engine aircraft, an airborne integration platform with batteries does not change its weight in flight (since no fuel is burned off), which will have a significant impact on structure and aerodynamics (see Section 6.2). The main

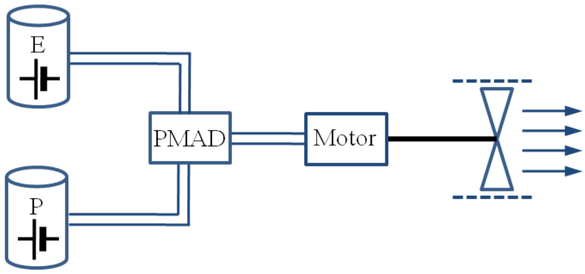

Fig. 3 U-ESA with batteries as only energy source.

performance penalty for purely electric power systems at the moment and in the foreseeable future is the high battery weight (see also Table 2). Technology advances in other mobility sectors an help to bridge the gap between the conflicting requirements of high energy and high power density, but step changes are necessary to make electric flight a reality beyond the scale of single-seater airplanes.

Table 2 Characteristics of battery-powered U-ESA.

Positive	Negative	Interesting
+ very high efficiency (∼90%)	- high battery weight	◦ recycling of batteries
+ no CG[a] movement	- landing weight same as take-off weight	◦ zero global emission possible
+ low maintenance	- small range	◦ replacement / recharging during turn-around
+ zero emissions in flight		

[a] Center of Gravity

4.2 Fuel Cell System

Figure 4 depicts the fuel cell power system; with its linear path from the hydrogen tank through the motor to the propulsor, this system is very similar to the conventional aircraft power plant, with kerosene replaced by hydrogen and the fuel cell instead of the turbo-engine. However, the efficiency of energy conversion is significantly higher for fuel cells. Note that in this system, there is mass change during flight due to fuel burn; however, because of the very low gravimetric density of hydrogen, energy storage contributes to the overall aircraft mass budget.

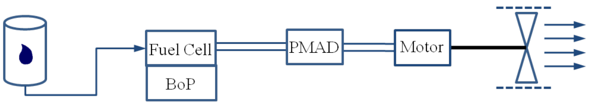

Fig. 4 U-ESA with fuel cell and hydrogen tank.

Table 3 Characteristics of fuel cell-powered U-ESA.

Positive	Negative	Interesting
+ higher efficiency + peak power fexibility of fuel cells	- H_2 tank integration - new fuel infrastructure needed	○ zero CO_2 possible ○ on-board use of produced water

4.3 Fuel Cell Battery Hybrid System

This hybrid system (see Fig. 5) combines the intrinsic advantages of the battery motor and the fuel cell system architectures. Notably, this system will profit from technology advances in both fields of research. Interesting synergies can be achieved by, for example, using the batteries as an emergency power source in case of fuel cell failure or by the fact that the cooling architecture of the hydrogen storage may be beneficially extended to superconducting PMAD components.

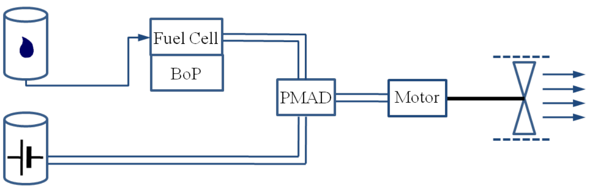

Fig. 5 U-ESA with hybrid hydrogen-supplied fuel cell and batteries.

4.4 Battery Turbo-Engine Hybrid System

In view of the analysis to be performed in Section 6, as a final example we discuss a hybrid of a battery-powered U-ESA with a conventional turbo-engine. The corresponding system is shown in Fig. 6. While any system using conventional combustion for power generation must miss the ultimate goal of zero in-flight emissions, this hybrid solution offers a feasible solution to the range loss problem caused by high U-ESA component weights. In Section 6, where notably we will introduce the Degree of Hybridization (DoH) to characterize the amount of power provided through each power conversion path.

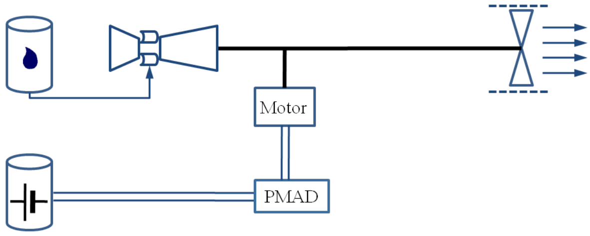

Fig. 6 Parallel hybrid system architecture with battery and conventional turbo-engine.

Table 4 Characteristics of battery turbo-engine parallel hybrid system.

Positive	Negative	Interesting
+ higher efficiency than conventional turbo-engine + fuel system and infrastructure partially unchanged	- weight penalty of PMAD, motor and batteries	○ integration-dependent structural benefits ○ noise reduction

5 Requirements for Future Electric Aircraft

Transport aircraft employing electro-mobility as a means of motive power have the benefit of realizing zero-emissions for both ground maneuvering and in-flight operations. Notwithstanding this desirable outcome, the detrimental effect of dramatic range reduction compared to the operational reach afforded by gas-turbine propulsion systems today makes the engineering systems trade-off prohibitive. The excessive weights of electro-mobility based solutions are attributable to high specific

Fig. 7 The CeLiner platform upon which all U-ESA sub-systems were designed.

weights of components that describe the integrated system, i.e. energy source (whether battery-only, fuel-cell-only, or a combination of the two), controllers, wiring and associated buses/connectors, and motors. Unfortunately, studies show that this penalizing circumstance cannot be effectively traded away by the rather high component efficiencies inherent to them. In this context, since weight is at a premium, a means of off-setting the detrimental effects of high take-off/landing regulated weights and en route flight gross weights would be to maximize low-speed and high-speed lift-to-drag ratios as well as find a means of improving the structural weight efficiency of the aircraft.

5.1 Mission Requirements

In order to perform the requisite array of sub-systems engineering trade-studies, the CeLiner was procured [5], which allowed to address sizing sensitivities and establish robustness. The aim was to understand the potential for scalability of the required technologies and at the same time encourage their propensity for evolutionary development. For purposes of showing characteristics associated with electro-mobile transport aircraft solutions, a pre-concept design of a 190-passenger aircraft aimed primarily at the short-haul market was synthesized (see Fig. 7). Exceeding Flightpath 2050 goals [4], the unique feature of this initial technical assessment activity was to produce a commercial transport that delivers zero-emissions from gate to gate. Entry-into-Service (EIS) for the baseline was set as year 2035.

This ambitious zero-emissions target was achieved through implementation of a Universally-Electric Systems Architecture (U-ESA), which includes a propulsion solution solely powered through electrical means. Advanced Li-ion batteries constitute the only source of electrical power. The batteries have been configured as modular packs that fit into suitably modified LD-3 containers in order to facilitate expedient turn-around and aid loadability. With regards to motive power the design proposal utilizes ducted fans run by High Temperature Superconducting (HTS) electric motors reflecting posited performance based upon test-rig data obtained from the literature [20, 21].

An innovative C-Wing morphology, dispensing with the need for a dedicated horizontal tailplane as well as maximizing vehicular aerodynamic efficiency, was selected due to airport compatibility requirements that imposed a span limit. Also, for purposes of ensuring compliance with contemporary standards of Configuration, Maintenance and Procedures (CMP), a complete aircraft systems design adhering to 90min Extended Twin OPerationS (ETOPS) was stipulated. This last technical requirement infers the U-ESA system needs to be supplied by at least three independent sources of power.

5.2 Universally-Electric System Requirements

The contemporary approach to electrical systems integration, the so-called ‘more-electric’ and the ‘all-electric’ architectures, irrespective of the extent of electrification require fundamentally mechanical off-take from a gas-turbine power source. Over time, incremental improvements will be achieved through wholesale application of Direct Current (DC) only power transmission. Apart from the principal advantage of improving power loss reduction through increased voltages, DC systems minimize electro-magnetic interference and are compatible with battery and/or fuel-cell energy sources since no specialized (and heavy) equipment for conversion to-and-from Alternating Current are required.

One engineering proposal for future ubiquitous electrical systems architectures is the U-ESA. The U-ESA is divided into three different main systems, all representing different power and voltage sources. The first level, dedicated to the propulsion system, is characterized by high power and voltage. The second level caters to onboard customer system requirements: i) non-essential, e.g. galleys; ii) essential, e.g. flight control; and iii) vital, e.g. emergency lights. This is associated with a medium power and voltage. The third level, with relatively low power and voltage demand feeds the avionics equipment.

6 Technology Gaps and Future Electric Air Transport Perspectives

It has been stated earlier that propulsion based upon the precepts of electro-mobility suffer from vehicular efficiency degradation due to relatively high specific weights of U-ESA-type components, thereby producing less than desirable operational reach, namely, range. It was deemed appropriate to perform a design perturbation study with intent to show the relative merits of implementing propulsion system solutions comprising a varying mix of gas-turbine and HTS motor for a requisite thrust. The following section offers details about the problem formulation behind this design perturbation and sensitivity study, and more importantly, offers a number of salient conclusions that can be drawn from the results.

6.1 Hybridization Degree of Freedom

In order to identify degrees of freedom for extenting the limited range of electrically powered aircraft, a hybridization study was performed. To this end, the universally-electric, short-range, medium-capacity aircraft concept CeLiner was hybridized through additional conventional energy storage and conversion, i.e. kerosene fuel and turbo-shaft gas-turbines partially delivering the required energy and power for the aircraft (compare Fig. 6).

CeLiner reflects technology status 2030 in terms of aerodynamic and structural performance. The energy and propulsion system of the reference aircraft comprises two installed power plants, an ETOPS compatible PMAD and battery system. The installed power plants consist of the bare HTS electric motors, the required cryocoolers and motor controllers, as well as the propulsive devices including the fan components, the fan drive gear boxes and the nacelles. The maximum take-off weight (MTOW) share of the overall energy and propulsion system is 42.8%, while the maximum structural payload is 19.0% of MTOW.

For the hybridization study, MTOW, structural weights and aerodynamic properties were kept fixed, equal to the reference aircraft, thereby, neglecting potential structural synergies or drawbacks due to the varying overall system architecture. With the assumption made, the overall installed power was considered invariant for the different aircraft investigated.

For the sizing of the individual components of the energy and propulsion system the individually required maximum powers were considered as significant. The corresponding critical sizing cases are indicated in Table 5.

Table 5 Summary of component modelling for hybrid energy and propulsion system.

	Sizing Case	Efficiency	Power Density	Energy Density
Battery[a]	take-off, AEO[c]	const	const	const
PMAD[a]	take-off, AEO[c]	const	const	n/a
HTS motor[b]	take-off, OEI[d]	const	$f(P_{\mathrm{el}})$	n/a
Gas-turbine	take-off, OEI[d]	$f(P_{\mathrm{co}})$	$f(P_{\mathrm{co}})$	n/a
Fuel	n/a	const	n/a	const

[a] incl. redundancies for ETOPS
[b] incl. cryocooler and controller
[c] All Engines Operational
[d] One Engine Inoperative

In the study, the degree of hybridization, H, was defined, expressing the share of installed power between electrical, P_{el}, and conventional, P_{co}, systems:

$$H = \frac{P - P_{\mathrm{el}}}{P_{\mathrm{co}} - P_{\mathrm{el}}}, \quad \text{where } P = P_{\mathrm{co}} + P_{\mathrm{el}}. \quad (1)$$

All components of the energy and propulsion system were sized according to the corresponding share of overall required power. The component efficiencies and power densities, i.e. power per component mass, were expressed as functions of the individual sizing powers. The specific power characteristics versus installed power for HTS motors were taken from Masson *et al.* [20, 21] and extrapolated to technology 2030+. The specific power of battery and PMAD system was treated constant for variations in power sizing. Using the determined power densities, the masses of the energy transmission components, i.e. PMAD, electric motors and gas turbines, were determined. The sizing power of the battery system was treated as directly coupled to the PMAD system, i.e. mass and available energy from the battery system scale proportionally with PMAD sizing power. The residual mass budget for the overall energy and propulsion system was considered available as hybrid energy storage, i.e. kerosene fuel and turboshaft engines adding to power of driving the propulsive devices. The masses and efficiencies of the propulsive devices were considered unaffected due to invariant aircraft thrust requirements. The efficiencies of the electrical system components were assumed independent from sizing power variations, in the first instance.

The dependency of turbo-shaft engine power density on installed power was mapped based on an empirical correlation given in Ref. [22]. The correlation was calibrated to match advanced engine characteristics in the relevant shaft power class. The power density of fuel was considered unlimited while potential tank and fuel system masses were accounted for within the chosen value of fuel energy density.

Aircraft range was calculated using the Brequet equation, extended for hybrid energy, based on the available exergies of the energy storage media and the corresponding individual mass losses during flight mission.

The integrated results of the study are shown in Figure 6.1, including aircraft range and stored exergy, as well as, CO_2 emissions and energy consumption per passenger and 100 km. This figure offers some interesting insights when it concerns selection of DoH in the context of passenger transport propulsion integration. At first glance it can be observed that the rate reduction in range capability for increasing level of electrification (represented by the DoH values tending towards zero) is non-linear tending towards vanishing slope.

As a primary effect, the rate reduction in range is directly proportional to the reduction in total available exergy of the turbo-electric system, since the available exergy from kerosene is an order of magnitude larger than what can be drawn from a battery based energy source. Other aspects that come into consideration are effects related to higher Instantaneous Gross Weights (IGWs), which is a bi-product of increasingly electrified propulsion system installations, i.e. PMAD versus fuel system, and the lower power density of installed HTS motors vs. advanced gas-turbines.

For turbo-electric power mixes of $H \leq 0.35$ (65% HTS motor and 35% gas-turbine for installed thrust), the rate reduction in range tends to diminish noticeably, i.e. less range loss with increasing amount of electrification. This can be explained by the interaction of steadily increasing hybrid system efficiency (diminishing gas-turbine efficiency due to scale effects versus a constant HTS motor efficiency), reduction of the penalizing impact of high IGW (PMAD weight increase offset by steadily improving HTS motor power density), and, increasing available exergy from the batteries.

Regarding the CO_2 per PAX$\cdot$100 km emissions trend with diminishing DoH, one can observe that parity occurs for turbo-electric hybrids of around 50% ($H = 0.50$) with that of the all-gas-turbine ($H = 1.0$). A 50% mix of turbo-electric propulsion yields range capability of around 3000 nm. For typical narrow-body aircraft this constitutes a very reasonable level of operational reach. It is highlighted that the all-gas-turbine solution corresponds to an evolutionary internal combustion propulsion system that already delivers approximately 25% improvement over the year 2000 state-of-the-art. The weak impact of DoH until the 50% mix point indicates that propulsion systems biased towards all-gas-turbine installations have no discernible benefits in the context of emissions - only yielding a detriment in terms of range capability.

If one now considers a CO_2 per PAX$\cdot$100 km emissions target in-line with propulsion-only expectations according to Flightpath 2050 [4], namely, a total reduction of 40% compared to the year 2000 datum [23], this corresponds to around

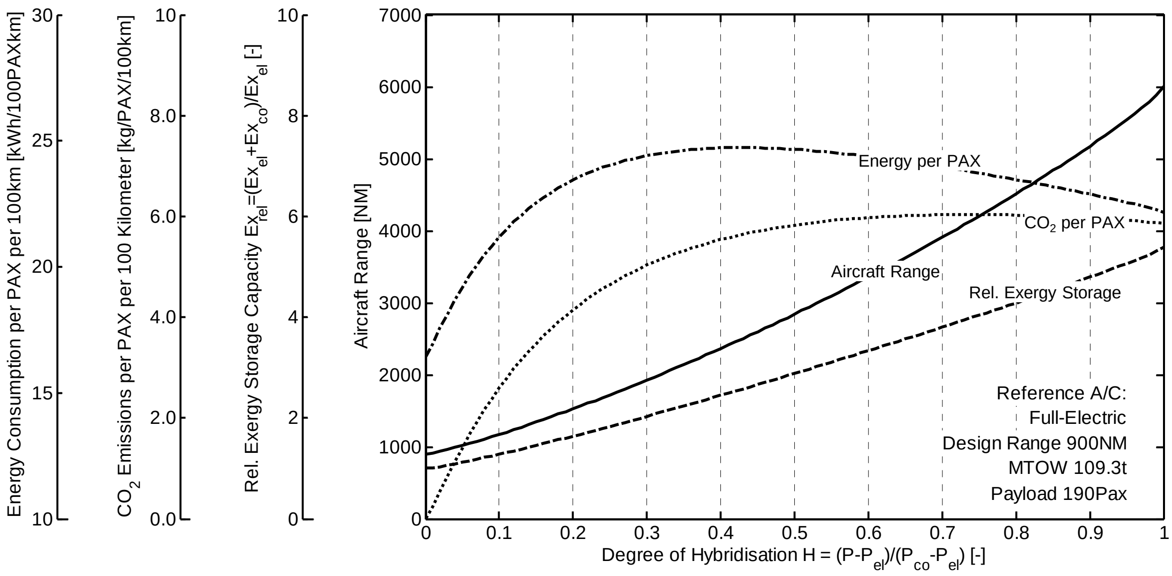

Fig. 8 Degree of hybridization for a parallel hybrid of gas-turbine and electric system; $H = 1.0$ denotes all-gas-turbine and $H = 0$ denotes universally-electric propulsion.

$H = 0.25$ (75% HTS motors and 25% gas-turbine for requisite thrust) and range capability of approximately 1750 nm. Beyond this, if it is assumed the propulsion system alone should deliver Flightpath 2050 goals, i.e. a 75% reduction in CO_2 per PAX·100 km, this corresponds to an operational reach of just over 1000 nm. Finally, based on the presented study, a full electro-mobility solution, that is to say zero-emissions in flight, would produce a range capability of 900 nm.

In summary, it can be concluded that $H = 0.25$ would meet the propulsion-only targets set by Flightpath 2050 (40% reduction compared to year 2000 datum) and still produce a reasonable maximum range (1750 nm) for the category of transport aircraft presented in this investigation. It is our view that if the ambition is to realize an even greater reduction in CO_2 per PAX·100 km, the trade-off between hybrid system complexity and range potential is not sufficiently in favor of hybrid turbo-electric solutions, and thus an all-electric propulsion system design should be considered if improved architectural solutions for hybrid energy and propulsion systems are not available.

6.2 Impact of Structural and Aerodynamic Efficiency Improvements

A prediction algorithm suited for the pre-design stage of transport aircraft design sizing was applied to the DoH study in order to gauge the relative merits of improved structural and/or aerodynamic efficiencies. The prediction method is a combination of statistical correlations of design variables and macro-objective functions with fractional change analytical constructs [24]. The analytical component of the fractional change method operates with the underlying premise that the designer/analyst begins with a seed condition or aircraft. Briefly, by considering an increment in variable x as dx or Δx, a fractional change to a new value, x_1, small or otherwise, in a seed parameter x_0 is defined as

$$\lhd x = \frac{\Delta x}{x_0} = \frac{x_1 - x_0}{x_0} \qquad (2)$$

Now, derivation of an integrated range model begins with the Breguet equation for range (R). In differential form the Breguet equation accounts for the change in aircraft instantaneous gross weight, W, based on an instantaneous specific air-range. One variation of the differential equation for range is to express it as a function of fuel calorific value, H_c, the overall power plant efficiency, η and the vehicular lift-to-drag ratio, (L/D), i.e.

$$dR = \frac{H_c}{g}\,\eta \cdot (L/D)\,\frac{dW_{\text{fuel}}}{W}\,. \tag{3}$$

Eq. 3 quotes only increments in range for an instantaneous condition. The actual aim is to seek an integrated range result wherein the product of $\eta \cdot (L/D)$ continually varies for the entire mission. One method is to assume an arbitrary reference point such as Initial Cruise Altitude (ICA) is related to the Takeoff Gross Weight (TOGW), where $W = k_{\text{clb}} \cdot TOGW$, $k_{\text{clb}} < 1$, and incorporate a profile correction (Θ_{prf}) that captures step-cruising as well as continually varying $\eta \cdot (L/D)$ effect. The profile correction coefficient value will be unique depending on the relationship between W at the ICA and the IGW at end of mission. In view of this association and since account is made for W at initial cruise in Eq. 3, it is reasonable to conclude that proportionality will exist between Θ_{prf} and Zero-Fuel Weight, i.e. 'ZFW = Basic Operating Weight (BOW) plus payload', and a suitable relationship has been established to be an exponential one, i.e. $\Theta_{\text{prf}} = (1 + \triangleleft ZFW)^{\epsilon}$. In order to permit an even wider scope of functional sensitivity with sufficient accuracy, an extension to the profile correction [24] would also include account of variations due to change in useful load as payload remains fixed, i.e. TOGW varies. This relationship was also found to be suitably represented by an exponential one with $\Theta_{\text{prf}} = (1 + \triangleleft\zeta_{\text{flt}})^{\alpha}$, where $\triangleleft\zeta_{\text{flt}}$ represents the flight fuel fraction, or,

$$\triangleleft\zeta_{\text{flt}} = \frac{(1 + \triangleleft W_{\text{flt}})}{(1 + \triangleleft TOGW)} - 1\,. \tag{4}$$

Upon introduction of an extended Θ_{prf} definition into the integration of Eq. 4, the method to quantify fractional change in range becomes

$$\triangleleft R = \frac{(1 + \triangleleft\eta)\,[1 + \triangleleft(L/D)]\,(1 + \triangleleft\zeta_{\text{flt}})^{\alpha}}{(1 + \triangleleft ZFW)^{\epsilon}} - 1\,. \tag{5}$$

Eq. 5 permits opportunity to perform sensitivity studies such that one can inspect the merits of increased structural efficiency (reduction in the ZFW variable) and higher aerodynamic efficiency (increase in (L/D) parameter). It should be noted that for an all-battery electro-mobility systems the exponents α and ϵ would be taken to be unity since for the IGW at any point during the flight is constant, i.e. equal to TOGW.

Figure 9 displays the functional sensitivity of R associated with arbitrary variations in ZFW (or TOGW if $H = 0$ and an all-battery energy source is utilised) and (L/D). The chart is applicable for all candidate DoHs presented in Fig. 8. If, for instance, a $H = 0.25$ is assumed (recall discussion of Fig. 8 in Section 6.1), and, an aerodynamic efficiency of +10% together with a reduction in ZFW of -5.0% is considered, the range capability of this candidate propulsion system mix would increase by 17.8%. In other words, the range would increase by around 300 nm from the 1750 nm datum.

7 Conclusions

Electro-mobility currently is the focus of considerable research effort, in both the publicly funded and in the industrial domains. In this paper, we addressed several key questions of electric flight, at the fundamental as well as at the system integration level. We argued that three principles should be at the heart of any feasibility analysis pertaining to airborne electrical systems: i) Exergy (rather than energy) content is the parameter of choice to describe an energy carrier's usefulness for aviation. ii) This exergy density of the energy carrier must be assessed in combination with the power density acheived when using a particular power conversion system, yielding the combined system's Ragone metrics. iii) Several energy carriers and power conversion systems which separately do not allow to sustain a given aircraft mission may be integrated into a suitable hybrid electrical power architecture capable of performing this mission.

We further showed that the availabe state-of-the-art components for airborne electric systems and in particular their future technology perspectives provide a promising starting ground to set up highly efficient hybrid electrical power architectures (which we refer to as HEPAs), which – unlike conventional combustion engines – are not limited by, e.g., the Carnot efficiency. We illus-

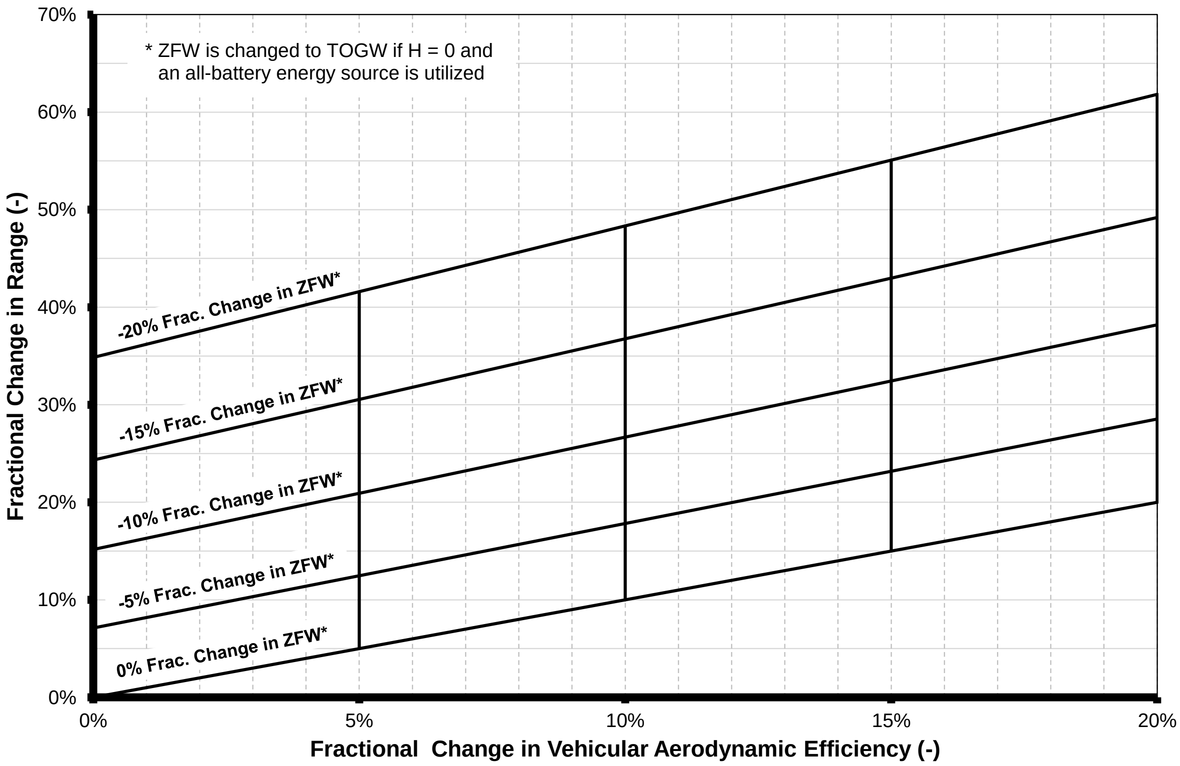

Fig. 9 Nomograph showing impact of structural weight and aerodynamic efficiencies on range.

trated four distinct HEPA realizations, including the Universally-Electric System Architecture (U-ESA), which has been implemented in our recent pre-concept design CeLiner [5].

Based on the CeLiner analysis, we concluded that the efficiency gains from electric flight can be truly optimized only if the entire solution space spanned by both the physical system properties and aircraft configurations is explored. In general, the increased weight of an airborne U-ESA platform entails a sizeable reduction in mission range; we therefore studied in detail a hybrid system of conventional turbo-engine and battery, which, depending on its degree of hybridization, allows for significant range extension, at the price, however, of losing the U-ESA's zero inflight emission property. Interestingly, our analysis shows that there is a threshold DoH, i.e. a minimum fraction of the aircraft power demand that must be contributed by the battery system, below which the hybridization benefits do not warrant the increased system complexity of the parallel gas-turbine and electric hybrid. In order to mitigate the drawbacks of this complexity, improved architectural solutions for hybrid energy and propulsion systems should receive increased attention.

In light of this work, we conclude that progress in electric air transport is advancing at a fast pace, offering bright perspectives in the medium- to long-term future. However, one must ensure the right tools are used to steer and quantify scientific developments, and a reliable physics-based modelling approach should be applied to all components and sub-systems as well as the resulting integrated aircraft concept.

References

[1] S. Naundorf et al. *Alternative Fuels for Aviation: Progress, Prioritization and Perspectives.* Proceedings of the German Aerospace Congress (DLRK), Bremen, Germany, Document ID 241439, pp. 1021-1026 (2011).

[2] H. Kuhn et al. *Renewable Energy Perspectives for Aviation.* Proceedings of the 3^{rd} CEAS Air&Space Conference and 21^{st} AIDAA Congress, Venice, Italy, pp. 1249-1259 (2011).

[3] A. Sizmann. *Neue Energieperspektiven der Luftfahrt*. IPICC Conference 'Fuelling the Climate 2010', Hamburg, Germany, June 18th, 2010.

[4] European Union. *Flight Path 2050. Europe's Vision for Aviation*. Brussels, Belgium (2011).

[5] Visionary Aircraft Concepts Group. *Concept 002: Initial technical assessment of an electrically-powered, medium-capacity, short-haul transport aircraft*. Internal Report IB-12021, Bauhaus Luftfahrt e.V., 2012.

[6] B. Kang, G. Ceder. *Battery materials for ultrafast charging and discharging*. Nature **458**(7235), pp. 190-193 (2009).

[7] C. Ban et al. *Extremely Durable High-Rate Capability of a $LiNi_{0.4}Mn_{0.4}Co_{0.2}O_2$ Cathode Enabled with Single-Walled Carbon Nanotubes*. Advanced Energy Materials **1**(1), pp. 58-62 (2011).

[8] Y.Yang et al. *New Nanostructured Li_2S/Silicon Rechargeable Battery with High Specific Energy*. Nano Lett. **10**(4), pp. 1486-1491 (2010).

[9] C.K. Chan et al. *High-performance lithium battery anodes using silicon nanowires*. Nature Nanotechnology **3**(1), pp. 31-35 (2008).

[10] L.F. Cui et al. *Carbon-Silicon Core-Shell Nanowires as High Capacity Electrode for Lithium Ion Battery*. Nano Lett. **9**(9), pp. 3370-3374 (2009).

[11] L.F. Cui et al. *Crystalline-Amorphous Core/Shell Silicon Nanowires for High Capacity and High Current Battery Electrodes*. Nano Lett. **9**(1), pp. 491-495 (2009).

[12] M.H. Park et al. *Silicon Nanotube Battery Anode*. Nano Lett. **9**(11), pp. 3844-3847 (2009).

[13] T. Song et al. *Arrays of Sealed Silicon Nanotubes As Anodes for Lithium Ion Batteries*. Nano Lett. **10**(5), pp. 1710-1716 (2010).

[14] H. Kuhn, A. Sizmann. *Fundamental Prerequisites of Electric Flying*. Proceedings of the German Aerospace Congress (DLRK), Berlin, Germany, submitted (2012).

[15] E. Middelman et al. *Bipolar plates for PEM fuel cells*. J. Power Sources **118**(1-2), pp. 44-46 (2003).

[16] D. Wang et al. *Highly Stable and CO-tolerant Pt/TiWO Electrocatalyst for Proton Exchange Membrane Fuel Cells*. J.Am.Chem.Soc. **132**(39), pp. 10218-10220 (2010).

[17] V. Mazumbder et al. *Core/Shell Pd/FePt Nanoparticles as Active and Durable Catalyst for Oxygen Reduction Reaction*. J.Am.Chem.Soc **132**(23), pp. 7848-7849 (2010).

[18] S. Moghaddam et al. *An inorganic-organic proton exchange membrane for fuel cells with a controlled nanoscale pore structure*. Nature Nanotech. **5**(3), pp. 230-236 (2010).

[19] K. Sivasubramaniam et al. *Development of a High Speed HTS Generator for Airborne Applications*. IEEE Trans. on Applied Superconductivity **9**(13), pp. 1656-1661 (2009).

[20] P.J. Masson et al. *HTS Motors in Aircraft Propulsion: Design Considerations*. IEEE Trans. on Applied Superconductivity **15**(2), pp. 2218-2221 (2005), trend information obtained from presentation given at ASC 2004, October 2004, Jacksonville, FL.

[21] P.J. Masson, C.A. Luongo. *High Power Density Superconducting Motor for All-Electric Aircraft Propulsion*. IEEE Trans. on Applied Superconductivity **15**(2), pp. 2226-2229 (2005).

[22] Hein et al. *Heavy Lift Helicopter*. College Park, MD, USA: Department of Aerospace Engineering, University of Maryland, 2005.

[23] Bauhaus Luftfahrt e.V. (coordinator). *Distributed Propulsion and Ultra-high By-pass Rotor Study at Aircraft Level*. Level 0 Collaborative Project, FP7-AAT-2012-RTD-L0, Proposal No. 323013 to the European Commission Directorate General for Research and Innovation, March 14th, 2012.

[24] A. Isikveren. *Parametric Modeling Techniques in Industrial Conceptual Transport Aircraft Design*. World Aviation Congress, Montreal, SAE Paper 2003-01-3052, September 2003.

8 Copyright Statement